ANALYSIS OF SHEARING INTERFEROGRAMS OF TEAR FILM USING FAST FOURIER TRANSFORMS

Tomasz J. Licznerski, Henryk T. Kasprzak, and Waldemar Kowalik
Technical University of Wroclaw, Institute of Physics, Wybrzeçe Wyspiański 27, PL-50-370 Wroclaw, Poland

(Paper JBO/IB-001 received June 18, 1997; revised manuscript received Oct. 20, 1997; accepted for publication Oct. 30, 1997.)

ABSTRACT

A new method for evaluating tear film stability on the human eye is reported. The tear film distribution on the cornea is measured by the lateral shearing interference technique. The eye is kept open during approximately a 2-min recording, when blinking has to be prevented. Continuous recording and viewing of interferograms allows the changes in disturbances of the interference fringes to be registered during elapsed time. The changes in fringes are caused by the evaporation of tears from the ocular surface and appearance of the breakups. For precise and repetitive assessment of the tear film breakup time, a fast fourier transform (FFT) is applied to consecutive interferograms. Larger fringe disturbances result in wider Fourier spectra. The tear breakup time can be evaluated noninvasively by comparing the value of the second momentum of Fourier spectra calculated from the consecutive interferograms. *© 1998 Society of Photo-Optical Instrumentation Engineers.* [S1083-3668(98)01301-X]

Keywords shearing interferometry; tear film breakup; tear film stability; NITBUT; FFT.

1 INTRODUCTION

The stability of the tear film over the cornea (or the contact lens) plays an important role in the condition of vision for optical and physiological aspects. The continuous three-layer structure of the tear film is sustained by involuntary periodic blinking. The blink movement ensures the formation of a continuous and smooth cover over the corneal surface. A typical interblink period ranges from 5 to 10 s.[1] If the eye is kept open for a longer time, the stability of the tear film is threatened and breaks with a random distribution in the continuous lacrimal film appear. Usually the tear film breakups form first over the corneal surface, where the tear layer is thinner, which results in the appearance of increasingly dewetted areas on the epithelium.[2] The mechanism of breakup is still unclear and has been investigated by many authors.[1–4] By measuring a time interval between the last eye blink and the first appearance of the breakup, useful information can be obtained on tear film stability. Norn[5] called this time interval ''corneal wetting time.'' Later, Lemp[6] proposed the name ''breakup time'' (BUT), but in fact the two terms are synonyms.

The slit lamp is usually used to observe tear film rupture and to evaluate BUT. In this method, an instillation of fluorescein is necessary to observe breakup formation. Unfortunately, the instillation introduces errors in BUT values.[5,7] Because of the use of fluorescein, the BUT value measured by this method is called the fluorescein breakup time (FBUT).

Menger et al.[7] describe a noninvasive instrument for assessing the precorneal stability of tear film. The instrument consists of a hemispherical bowl attached to a binocular slit-lamp microscope. The pattern inside the bowl is projected onto the eye and reflected from the air–tear boundary. If the tear film is distorted, the reflected image becomes discontinuous. The elapsed time (in seconds) between the last complete blink and the first appearance of discontinuity in the reflected pattern has been called a noninvasive tear breakup time (NITBUT). Despite the great improvements in BUT measurements which lie in eliminating fluorescein instillation and lowering light intensity, this method still has some disadvantages. First, NITBUTs are subjectively found by the observer, who judges whether there are discontinuities or not. Second, only the areas that reflect a grid pattern are tested. These two facts can influence the NITBUT data.

One of the methods that meets the need for noninvasive testing of the tear film, and that has the possibility of precise and repeatable measurements, is interferometry. One of the first optical methods that uses interferometry for measuring the axial

Address all correspondence to T. J. Licznerski. Tel. (4871) 320 36 13; Fax: (4871) 22 96 96; E-mail: tomo@rainbow.if.pwr.wroc.pl

1083-3668/98/$10.00 © 1998 SPIE

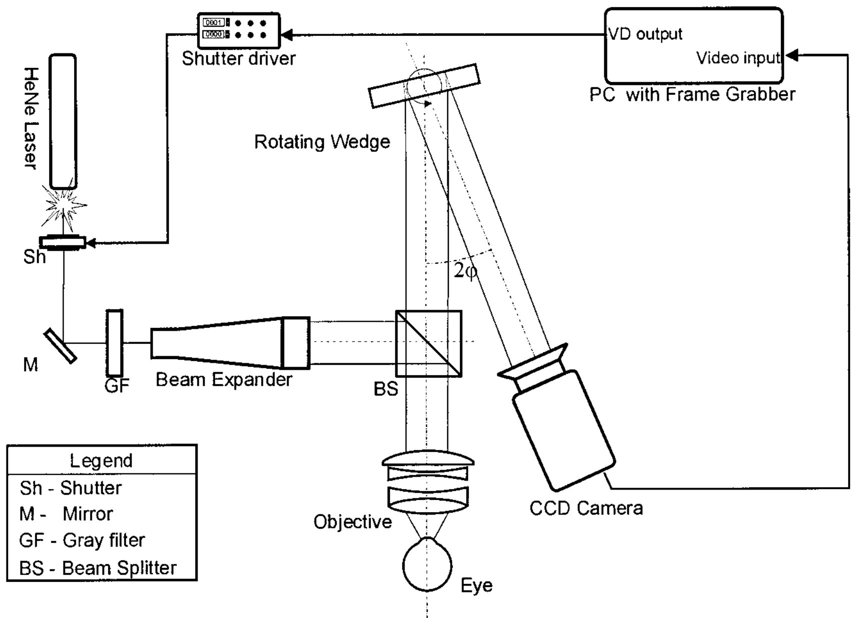

Fig. 1 The schematic setup of the lateral shearing interferometer.

length of the human eye was proposed by Fercher, Mengedoht, and Werner in 1988.[8] In 1993, Kasprzak, Kowalik and Jaroñski[9] proposed an interferometric setup for corneal topography measurements. The setup can also be used as a tear film stability screening method, which is reported in Refs. 10 and 11. Although this method is very precise, it also has some drawbacks. One of them is the difficulty of aligning the eye to the axis of an interferometric setup.

This paper describes a shearing interferometric method for tear film stability measurements and automatic evaluation of NITBUT. The method is less sensitive than the Twyman–Green interferometer used in Refs. 9 through 11 but allows more freedom in the eye alignment. An automatic method for the evaluation of the interferograms obtained is also described.

2 METHOD

The interference fringes in the lateral shearing technique (LST) correspond to the differences in optical paths between shifted wavefronts. The shift of the wavefronts can be obtained by many techniques. In the method described here, the shift is introduced by a wedge inserted in the optical path as shown in Figure 1. The top and side views of the wedge with the incident and reflected rays are presented in Figure 2. The wedge was designed to have an internal angle of about $\alpha=30$ deg and is placed in the setup to have an angle of approximately $\varphi=15$ deg between the normal to the surface of the wedge and the wave propagation axis. This arrangement ensures both the lateral and the angular shifts between the wavefront incident on the wedge (W_i) and reflected from its rear surface, and the wavefront that is reflected from the front surface (W_r). Moreover, it also allows us to alter the shearing parameter by rotating the wedge as indicated in Figure 1. In this case, an increase of the shear parameter increases the carrier frequency.

The shape of the wavefront carries information about the surface of the tear–air interface. If the tear film is continuous and smooth, smooth and almost parallel fringes are observed. However, when the eye is kept open for a long time and breakups occur in the tear film, the wavefront reflected from the tear film surface becomes distorted. This results finally in distortion of the interference fringes. The distortion of the carrier frequency in the fringe pattern is then examined by applying two-dimensional fast Fourier transform (FFT) to the image.

The second momentum is then calculated from the first order in the Fourier domain. The calcula-

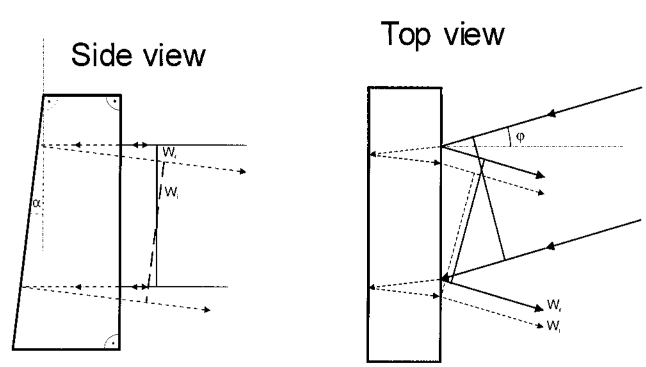

Fig. 2 Side and top views of the wavefronts on the wedge. W_r represents the wavefront reflected from the first surface of the wedge, and W_i is the wavefront incident and reflected from the rear surface of the wedge.

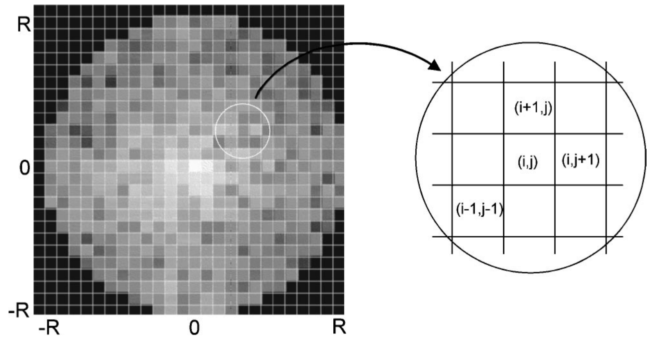

Fig. 3 Matrix of the first-order Fourier spectrum selected from the Fourier-transformed interferogram. Right: the method of accessing the matrix elements by use of i and j indices for calculation of the second momentum of the first Fourier spectrum.

tion of the second momentum is repeated for continuously recorded interferograms. If the value of the second momentum increases, it means that the breakup appears in the tear film. NITBUT can be evaluated by measuring the time interval between the complete eye blink and the moment of observed increase of the value of second momentum. The corneal topography is a part of the value of the second momentum calculated from the interferogram but it is a constant component in comparison with the part that is introduced by changes in the tear film deterioration.

To minimize the influence of spherical aberrations of the collimating lens in front of the eye on the calculations, and to reduce the processing time, a middle section of the interferogram was taken for further processing. An area 256×256 pixels square was chosen and the two-dimensional FFT of this section was calculated.

The first harmonic in the Fourier domain is selected by searching for the highest intensity points (HIP) of the spectrum. The intensity I is calculated as follows:

$$I=|\text{imaginary}(S)|^2+|\text{Real}(S)|^2, \tag{1}$$

where imaginary=the imaginary part of the Fourier spectrum; Real=the real part of the Fourier spectrum; and S = the matrix where the first Fourier spectrum is stored.

Before the HIP is selected, the zero-order harmonic is masked. If the HIP is found, the surrounding points within a certain radius R from the HIP are taken for the calculations of the second momentum M of the intensity I in relation to HIP. Figure 3 presents the first-order Fourier spectrum selected from a 2-D Fourier domain. The spectrum selected is placed in the matrix S and the second momentum is calculated. The indices i and j of matrix S are used to access the matrix elements. The method of indexing the matrix S is shown in Figure 3.

The intensity I for each point is multiplied by the square of its distance to the HIP and added together

$$M=\sum_{i=-R}^{i\leqslant R}\sum_{j=-R}^{j\leqslant R} I_{i,j}\times(i^2+j^2), \tag{2}$$

where I = the intensity calculated from Eq. (1), R = the radius of the Fourier spectrum; and i,j = the indices in matrix S of the size $2R\times 2R$.

It is known from the FFT properties that the single frequency results in two Dirac deltas (a larger value of HIP and a lower second momentum) presented in the Fourier transform domain. A more distorted carrier frequency makes the first-order spectrum flatter and more spread out (a lower value of HIP and a larger second momentum).

3 EXPERIMENT

The experimental setup of the lateral shearing interferometer and CCD camera is presented in Figure 1. We used (a 3-mW He:Ne laser as a source of coherent light in the experiment. The beam intensity is reduced when the eye is illuminated by gray filters and by applying an electromechanical shutter synchronized with a CCD camera. The vertical drive signal from the camera separated in a frame grabber card triggers the shutter driver. The time exposure can be adjusted by the shutter driver, which steers the shutter. The shutter releases 1-ms laser pulses, which are then directed to a collimator. The collimated laser beam, 30 mm in diameter, enters the interferometer. The beamsplitter directs the beam to the objective, which converts the plane wavefront to a spherical one. The collimated spherical wavefront falls on the cornea in such a way that the focus of the wavefront coincides with the center of the central corneal curvature. The wavefront reflected from the air–tear interface carries data about the tear film distribution over the cornea or contact lens. Passing back through the objective, the wavefront is reconverted and becomes quasiplanar again and then reaches a wedge.

The two wavefronts reflected from the front and the rear surfaces are superimposed and interfere. The pattern of interference fringes is recorded by the CCD camera. The images are digitized by the frame grabber card and stored in a computer memory for further image processing.

Our aim was to classify the interference patterns that correspond to the states of tear film deterioration. FFT provides a fast and reliable tool for such classification. The data from FFT together with the time interval between recorded images can be used to evaluate NITBUT.

The power of the laser light illuminating the cornea was less than 0.15 mW. The diameter of the illuminated corneal surface was about 5 mm. Thus the power density on the corneal surface amounted to less than 8 W/m^2. The laser pulses lasted 1 ms and were repeated at a frequency of 25 Hz over the 60-s time period of the continuous recording. This gives 60 s (recording time)×25 (pulses) ×0.001 s

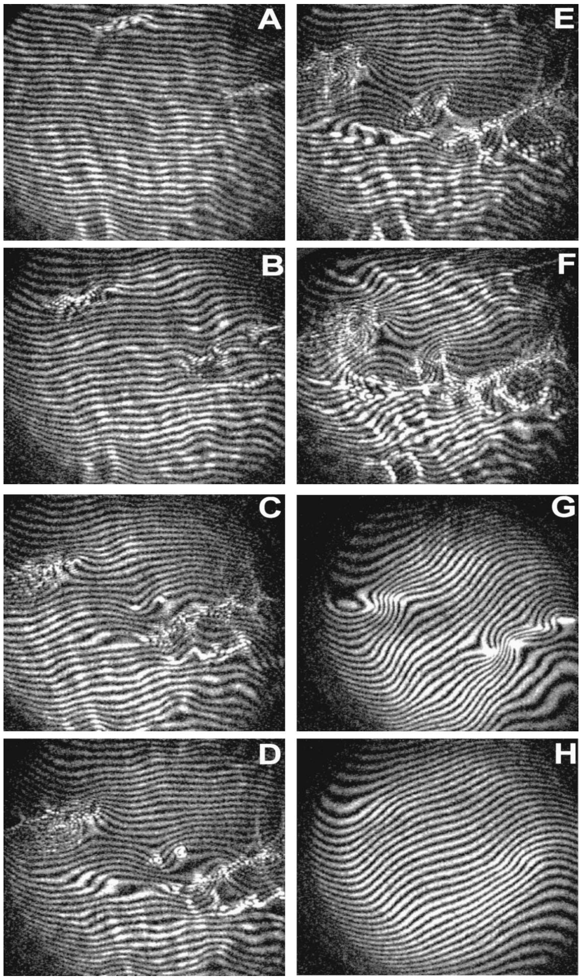

Fig. 4 A sequence of interferograms recorded at approximately 3-s time intervals. The first interferogram was recorded 10 s after the last eye blink. The eye was kept open for 25 s of recording. (a–f) The tear film disruption process is clearly visible, as indicated by the fringe pattern's deterioration. (g) The eye just after the eye blink. The tear layer does not recover entirely and the deformation of the fringes indicates locations of serious tear film damage. (h) The eye after several blinks 3 s later.

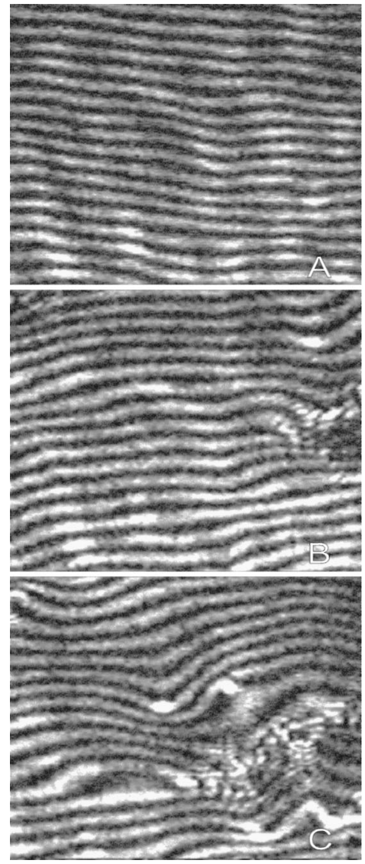

Fig. 5 The middle, 256×256 pixel areas selected for calculations from the interferograms in Figures 4(a) through 4(c).

(pulse width)=1.5 s of total illumination time, so the total illumination energy was 1.5 s (total illumination time) $\times 8\ \mathrm{W/m^2}$ (power density) $= 12\ \mathrm{J/m^2}$.

The single-pulse energy was 0.001 s (pulse width) $\times 8\ \mathrm{W/m^2}$ (power density)=$0.008\ \mathrm{J/m^2}$. This is below the allowed value for this wavelength (633 nm) and the exposure time.

4 Results

Figures 4(a) through 4(f) present a sequence of shearing interferograms showing the development of breakup on the normal eye during the interblink period. The time interval between the images is approximately 3 s.

The interference fringes from Figures 4(a) to 4(f) become more and more distorted due to the evaporation of the tears and formation of the breakups. The interferogram shown in Figure 4(g) presents the same tear layer after the eye blink. It is easy to see that one blink is not enough to restore a smooth tear cover over the cornea after serious disruptions in the tear film. Figure 4(h) shows the same eye interferogram after several strong blinks. This is how the interferograms of healthy and stable tear films should look after a blink.

An area 256×256 pixels square was chosen from the middle sections of the interferograms given in Figures 4(a) through 4(c) and is presented in Figures 5(a) through 5(c). The two-dimensional FFT of these pictures was calculated and is shown in Figures 6(a) through 6(c). The dark rings mark the area with the HIP in the middle and surrounding points taken for calculations. The black spots in the middle of the pictures represent a masked zero order. The amplitudes calculated from points within the rings are plotted in Figures 7(a) through 7(c). The high amplitudes in the middle of the marked rings correspond to the smoother fringe pattern. The low center amplitude and noisy surrounding correspond to the distorted fringe pattern.

The values of momentum calculated from Eq. (2) for the images presented are shown in Table 1. The columns contain the momentum values for different radii R of Fourier spectra taken for calculation. It is easy to see that the longer values of momentum

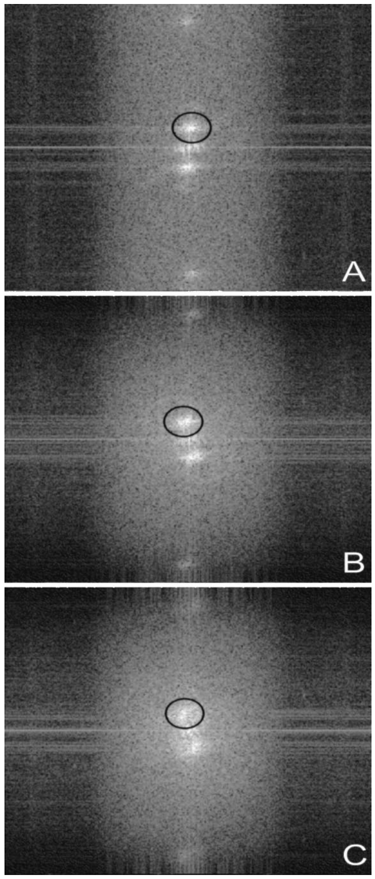

Fig. 6 The Fourier spectra of the selections presented in Figures 5(a) through 5(c). The dark rings surrounding the first-order Fourier spectrum are selected for the second momentum calculation. The HIP is in the middle of the ring on each image.

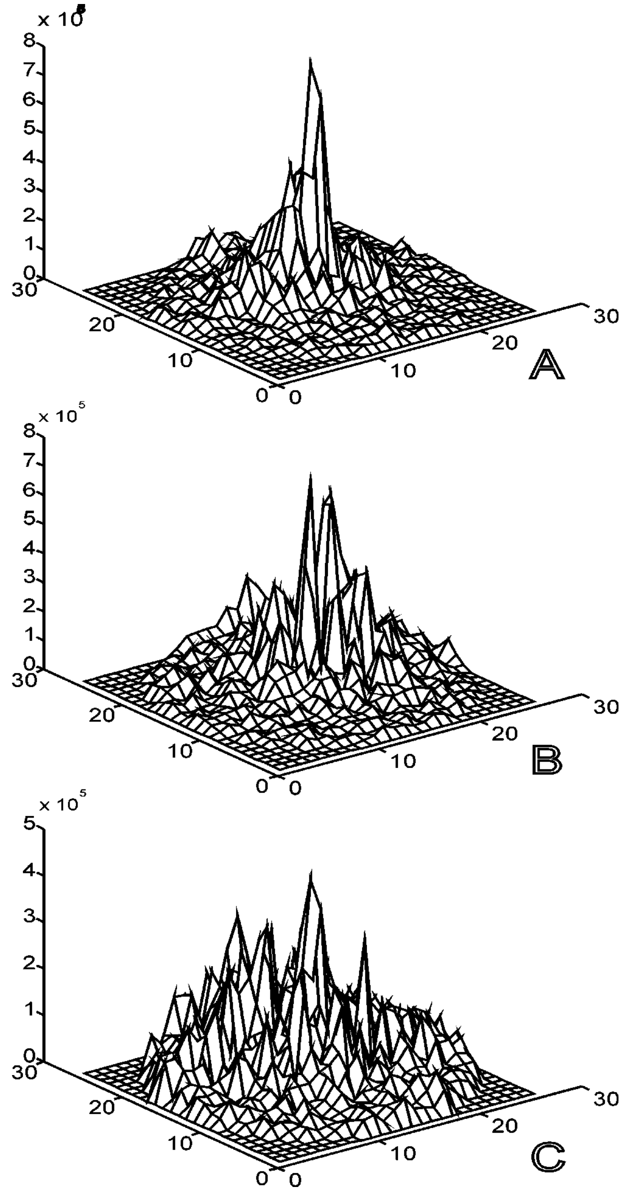

Fig. 7 3-D plots of intensities of the first-order Fourier spectra selected from Figure 5 help in understanding the interpretation of the value of the second momentum.

represent higher disturbances of the fringes that are directly related to the tear film disruptions. This fact is obviously the greatest advantage of this method, because it enables automation of the classification process. Thus the NITBUT calculation is much more reliable and measurements are more precise.

5 CONCLUSIONS

A new method for evaluating tear film stability has been introduced. The lateral shearing interferometer allows noninvasive testing of the human tear layer with a high accuracy. The FFT produces data that can be used for automatic processing of NITBUT calculations. Assessment of the tear film deterioration takes approximately 1–2 min and can be performed for both eyes. The noninvasiveness of

Table 1 The values of the second momentum $\times 10^9$ calculated for different radii R of the Fourier spectrum.

Figure	Second momentum values							
A	0.3398	0.4527	0.5826	0.7334	0.9103	1.1146	1.4208	1.6581
B	0.4875	0.6603	0.8531	1.0997	1.3309	1.7510	2.2707	2.6117
C	0.5248	0.7723	1.0910	1.5036	1.9008	2.4834	3.2173	3.7107
Radius R [pixels]	8	9	10	11	12	13	14	15

the method and the limited intensity of the laser light reduce reflex tearing. Thus NITBUT values can differ from standard FBUT ones. Areas of application of the method include dry eye diagnosis, testing artificial tears and contact lens wettability, and fitting contact lenses.

Acknowledgments

This study was supported by Research Grant No. 8T11E05310 from the Polish Committee of Scientific Research (KBN).

REFERENCES

1. A. Sharama and E. Ruckenstain, ''Mechanism of tear film rupture and formation of dry spots on cornea,'' *J. Colloid Interface Sci.* **106** (1), 12–27 (1985).
2. E. Ruckenstain and A. Sharama, ''A surface chemical explanation of tear film breakup and its implications,'' in *The Preocular Tear Film: In Health, Disease and Contact Lens Wear*, F. J. Holly ed., Chap. 63, pp. 697–727, Dry Eye Institute, Lubbock, TX (1986).
3. J. Holly, ''Formation and rupture of the tear film,'' *Exp. Eye Res.* **15**, 515–525 (1973).
4. P. Lin and H. Brenner, ''Stability of the tear film'' in *The Preocular Tear Film: In Health, Disease and Contact Lens Wear*, F. J. Holly ed., Chap. 60, pp. 670–675, Dry Eye Institute, Lubbock, TX (1986).
5. S. Norn, ''Tear film breakup time. a review,'' in *The Preocular Tear Film: In Health, Disease and Contact Lens Wear*, F. J. Holly ed., Chap. 3, pp. 52–55, Dry Eye Institute, Lubbock, TX (1986).
6. A. Lemp and J. R. Hamill, ''Factors affecting tear film breakup in normal eyes,'' *Arch. Opthalmol.* **89**, 103–105 (1973).
7. S. Mengher, A. J. Born, S. R. Tonge, and D. J. Gilbert, ''Non-invasive assessment of tear film stability,'' in *The Preocular Tear Film: In Health, Disease, and Contact Lens Wear*, F. J. Holly ed., Chap. 5, pp. 64–75, Dry Eye Institute, Lubbock, TX (1986).
8. A. F. Fercher, K. Mengedoht, and W. Werner, ''Eye length measurements by interferometry with partially coherent light,'' *Opt. Lett.* **13**, 186–192 (1988).
9. T. Kasprzak, W. Kowalik, and J. Jaroñski, ''Interferometric measurements of fine corneal topography,'' *Proc. SPIE* **2329**, 32–39 (1994).
10. J. Licznerski, H. T. Kasprzak, and W. Kowalik, ''*In vivo* measurements of the tear film on a cornea and a contact lens by use of interferometry,'' *Proc. SPIE* **2930**, 157–161 (1997).
11. J. Licznerski, H. T. Kasprzak, and W. Kowalik, ''Two interference techniques for *in vivo* assessment of the tear film stability on a cornea and a contact lens,'' *Proc. SPIE*, in press.